

# Light-induced change of magnetization of Bi-containing single-crystal iron-garnet films

A. M. Balbashov, B. A. Zon, V. Ya. Kupershmidt, G. V. Pakhomov, and T. T. Urazbaev

*Voronezh State University*

(Submitted 17 October 1987)

Zh. Eksp. Teor. Fiz. **94**, 304–314 (May 1988)

The change of the magnetization of rare-earth iron-garnet films of various compositions was experimentally investigated in a longitudinal magnetic field and in a range from room to Curie temperature. At relatively low temperatures, the magnetization of a number of films containing Lu and Yb is altered by nonthermal action of pulsed optical radiation. A theoretical analysis has shown that the nonthermal magnetization-change mechanism is due to field-governed factors in the Cotton-Mouton effect. An estimate is obtained of the time of longitudinal relaxation of the light-induced magnetization.

## 1. INTRODUCTION

Many theoretical and experimental studies have by now been devoted to the magnetization of various media in which optical radiation propagates.<sup>1</sup> The physical mechanisms responsible for such effects can be quite naturally divided into two groups. The first is connected with the light-induced change of the magnetization of transparent substances, when the real absorption of the light energy is low and plays no decisive role. The magnetization change can then be attributed to stimulated scattering of light by the atoms of the medium. This includes the inverse Faraday effect (IFE), which was investigated for diamagnetic substances<sup>2,3</sup> and for paramagnetic<sup>4,5</sup> and magnetically ordered<sup>6</sup> crystals, and the inverse Cotton-Mouton effect (ICME).<sup>7</sup>

The second group of mechanisms that give rise to light-induced magnetization is connected with the interaction between electromagnetic radiation and crystals in the region of an absorption band. Thus, in Ref. 8 was considered, in a Cotton-Mouton geometry, the change of the population of the magnetic sublevels of  $\text{Cr}^{3+}$  ions in a ruby crystal by interaction with resonant optical radiation and the ensuing appearance of induced magnetization. The change of the magnetization of magnetically ordered crystals was attributed in Refs. 9 and 10 to a change of the domain structure in the electromagnetic-radiation field by magnetic circular dichroism, and in Refs. 11–13 to piezomagnetic and magnetoelastic interactions and to a direct thermal (pyromagnetic-mechanism) change of the crystal's saturation magnetization. We mention also studies of magnetic semiconductors, whose magnetization change is attributed to variation of the indirect exchange by virtual transitions of the electrons and to the appearance of excitonic excitations,<sup>1,14,15</sup> and also studies of real photoabsorption by electrons of the valence band and of unfilled  $d$  and  $f$  shells.<sup>16,17</sup>

Observation of light-induced changes of the magnetization of transparent lutetium and ytterbium iron garnets by linearly polarized radiation—the inverse Cotton-Mouton effect—was briefly reported earlier in Ref. 18, where the effect observed was theoretically interpreted using a one-sublattice ferromagnet model.

We report here more detailed results. In particular, we have measured the temperature dependence of the magnetization change in the range from room temperature to the Curie point. The results have shown that at high tempera-

tures the predominant role is assumed by thermal effect, even though the films remain weakly absorbing. At room temperature, the decisive contribution to the change of the magnetization of a number of samples is made by the ICME.

The theoretical analysis casts light on the roles of thermomagneto-elasticity and pyromagnetism. Analysis of the ICME has shown that to explain the experimental results it is necessary to take into account, along with the parameters responsible for the direct Cotton-Mouton effect and for isotropic magnetic refraction, also the factors that lead to the field dependence of the magnetic refraction on the external magnetic field. The latter are weakly revealed by direct linear magneto-optic effects in low-strength external fields, and have not been observed in the direct Cotton-Mouton effect to this day. In the ICME, however, the role of these effects, as will be shown below, is predominant. The contribution of field quantities to the direct Faraday effect was investigated theoretically and experimentally in Refs. 19 and 20.

The next section of this paper is devoted to a description of the experimental setup and to the measurement procedure. In the third section we discuss qualitatively the form of the observed signal in the thermal and direct mechanisms of light-induced change of the magnetization. In the fourth we report the measurement results for various rare-earth iron-garnet films. The fifth section contains a theoretical description of the direct mechanism. In the concluding section we compare the theory with experiment and present numerical estimates.

## 2. EXPERIMENT

Light-induced magnetization was measured in thin (on the order of several microns) single-crystal Bi-containing iron-garnet films, with a common formula  $(\text{R}, \text{Bi})_3(\text{Fe}, \text{Ga})_5\text{O}_{12}$ , where R is the rare-earth ion or group of ions. In particular, we investigated films with  $\text{R} = \text{Lu}, \text{Yb}, \text{Tm}, (\text{LuSm})$ , having at room temperature saturation magnetizations in the range  $4\pi M_s \sim 420\text{--}200$  G. These films were grown by liquid-phase epitaxy on a (111) gallium-gadolinium-garnet (GGG) substrate.

The source of the intense electromagnetic radiation was a neodymium-doped YAG laser with the following output-radiation parameters: linear polarization  $\approx 99.9\%$ , emission wavelength  $\lambda = 1.06 \mu\text{m}$ , pulse duration at half-maximum  $\tau_L = 7\text{--}15$  ns, pulse repetition frequency 12.5 Hz, pulse en-

ergy  $\leq 0.015$  J, and cross section  $a$  of the beam bounded by an iris diaphragm of  $\approx 1.5$  mm diam.

Samples in the form of plates with surface area  $\approx 0.5$ – $1$  cm<sup>2</sup> were placed in the external magnetic field perpendicular to its force lines. The magnetic field was produced by a solenoid whose axis was aligned beforehand with the laser beam. The laser emission was normally incident on the sample surface.

When necessary, the radiation polarization could be varied with a  $\lambda/4$  plate. The energy of the incident pulses was measured by diverting, with a plane-parallel plate, a calibrated fraction of the radiation to an average laser-power and energy meter IMO-2N, and the pulse waveform was monitored by part of the radiation similarly diverted to an FK-19 high-speed photoelectric converter.

The sample magnetization was measured with a flat coil having three turns of thin copper wire and placed directly on the sample surface. By proper adjustment, the laser beam was incident through the coil center but did not overlap the turns. The signal from the measuring coil was fed through a broadband amplifier to an oscilloscope.

To estimate the temporal resolution of the recording system consisting of the measuring coil, the amplifier, and the oscilloscope we used a pulsed magnetic field produced between the central conductor and the braid of a coaxial cable by passage of a rectangular pulse.<sup>21</sup> The coil was placed in a narrow longitudinal slot out in the outer braid of the cable. For times comparable with the laser-pulse duration, a current pulse with subnanosecond rise time can be produced by inducing in the coil a delta-function-like emf. The measurable broadening of such a signal passing through the transmission line contains information on the time resolution of the recording system, found in our case to be  $\approx 3$  ns.

To keep out stray signals from the laser system, all the recording elements were thoroughly shielded. This lowered the parasitic-signal level to that of the amplifier noise observed on the oscilloscope, which was of the order of 60  $\mu$ V when referred to the amplifier input.

For measurements ranging from room temperature to Curie point, which did not exceed 200° C for all the investigated films, a miniature ceramic oven was placed inside the solenoid. The sample was secured in the oven to a heat pipe with an opening for passage of the beam. The temperature was measured with a thermocouple whose hot junction was placed on the heat pipe in the immediate vicinity of the crystal.

Since all the investigated films were grown on GGG substrates, special experiments were performed with pure GGG crystals, from which no signal was observed.

### 3. PROFILE OF SIGNAL EMF

The signal emf from the measuring coil is due to a change of the induction flux through the circuit around it. We assume for simplicity that the light-energy density is distributed uniformly over the laser cross section, in a circle of radius  $a$ . It can be assumed in this case that the film magnetization also varies uniformly in this circle. The flux induced by the magnetization  $\Delta M(t)$  is then equivalent to the induction flux from a straight round current  $J = c\Delta Mh$ , and is equal to<sup>22</sup>

$$\Delta \Phi = 4\pi \Delta M(t) (a+R) h \left[ \frac{a^2+R^2}{(a+R)^2} K(x) - E(x) \right],$$

$$x = \frac{2(aR)^{1/2}}{a+R}. \quad (1)$$

Here  $R$  is the coil radius,  $h$  the film thickness, and  $K$  and  $E$  complete elliptic integrals. It is assumed that the magnetization is constant along the film thickness, since in our case  $h \ll \alpha^{-1}$ , where  $\alpha$  is the radiation-absorption coefficient. Equation (1) takes in the limit  $a \ll R$  the simpler form

$$\Delta \Phi \approx 2\pi^2 \Delta M(t) \frac{a^2 h}{R} \equiv \gamma \Delta M(t). \quad (2)$$

We shall use this simpler equation hereafter. The terms omitted are small, of order  $(a/R)^2$ . To take them into account it is necessary to take simultaneous account of the real intensity distribution over the laser-beam cross section; in our case  $(a/R)^2 \approx 1/4$ .

It will be helpful in what follows to distinguish, as stated in the Introduction, between the direct magnetization change, due to the "instantaneous" action of the optical radiation, and the change due to the sample temperature rise. We can write for the light-induced crystal magnetization (which we designate  $\Delta M_I$ ) due to the direct mechanisms the phenomenological equation

$$\partial \Delta M_I / \partial t + \Delta M_I / \tau = \kappa I(t). \quad (3)$$

Here  $\tau$  is the relaxation time,  $I(t)$  the radiation intensity at the given instant of time, and  $\kappa$  a proportionality coefficient determined by the specific mechanism that connects the magnetization and the light intensity.

Equation (3) has the simple solution

$$\Delta M_I(t) = \kappa \int_{-\infty}^t \exp\left(-\frac{t-t'}{\tau}\right) I(t') dt'. \quad (4)$$

We consider two limiting cases. Let  $\tau_L$  be the characteristic laser-pulse variation time, i.e., a time during which  $I(t)$  changes noticeably. For  $\tau \ll \tau_L$  the intensity can then be regarded as constant and taken from under the integral sign:

$$\Delta M_I(t) = \kappa \tau I(t). \quad (5)$$

Thus, if the magnetization relaxation time is much shorter than the laser-pulse duration, the magnetization follows up adiabatically the radiation intensity. The signal emf has in this case the form of the derivative of the intensity:

$$\mathcal{E} = -\frac{1}{c} \frac{\partial \Phi}{\partial t} = -\frac{\gamma \kappa \tau}{c} \frac{\partial I}{\partial t}.$$

In the opposite limiting case  $\tau \gg \tau_L$  we obtain from (5)

$$\Delta M_I(t) = \kappa \int_{-\infty}^t I(t') dt'.$$

The signal emf has then the form of the laser pulse:

$$\mathcal{E} = -\gamma \kappa c^{-1} I(t).$$

We assume now that the magnetization change is due to a change of the crystal temperature  $T$  which is in turn varied in time by the action of the light. In this case

$$\Delta M = \frac{\partial M}{\partial T} \Delta T, \quad \Delta T(t) = \kappa' \int_{-\infty}^t I(t') dt',$$

$$\mathcal{E} = -\frac{\gamma \kappa'}{c} \frac{\partial M}{\partial T} I(t). \quad (6)$$

If the magnetization change is due to the sample temperature change, the observed emf is proportional to the radiation intensity. The quantity  $\kappa'$  in (6) is connected with the absorption and heat-capacity coefficients of the crystal. Obviously,  $\kappa' > 0$ , whereas (in our case)  $\partial M / \partial T < 0$ , so long as we are not in the vicinity of the compensation temperature  $T_c$ . In the latter case, however the contribution of the thermal signal should decrease with further temperature rise, and reverse sign, contrary to our measurement results. The proportionality of  $\mathcal{E}$  and  $I$  in (6) has therefore a positive coefficient.

In addition to the direct pyromagnetic mechanism  $\Delta_p$ , a magnetization variation  $\Delta_{me}$  with temperature can be produced by magnetoelastic interactions produced in the crystal by the onset of thermoelastic strains. The contribution of the latter mechanism, however, is small compared with the direct mechanism. Let us estimate  $\Delta M_{me}$  in the static limit  $\tau \ll \tau_L$ . Obviously, the allowance that must be made for the magnetization relaxation at  $\tau \gtrsim \tau_L$  does not change the order of magnitude of the result. The magnetoelastic part of the free energy is of the form<sup>23</sup>

$$F_{me} = B_{ijkm} M_i M_j u_{km} / M_s^2,$$

where  $B_{ijkm}$  is the magnetoelastic-coefficients tensor,  $u_{km}$  the elastic-strain tensor, and  $M_s$  the saturation magnetization. This form of  $F_{me}$  amount  $\Delta K_{ij} = B_{ijkm} u_{km}$ . The change of the  $\Delta M_{me}$  z-component recorded in experiment is due both to the  $\mathbf{M}(\mathbf{H})$  dependence

$$\Delta \mathbf{M}_{me}^{(1)} = -\partial F_{me} / \partial \mathbf{H},$$

and to the change, which we designate  $\Delta \mathbf{M}_{me}^{(2)}$ , of the direction of the vector  $\mathbf{M}$  as a result of  $\Delta K_{ij}$ . In the static limit, under the condition  $H_a \gg H - 4\pi M_s$ , where  $H_a$  is the uniaxial anisotropy field, it is easy to obtain the estimates:

$$\Delta M_{me}^{(1)} \sim \chi B u_{ij} / M_s, \quad \Delta M_{me}^{(2)} \sim M_s (\Delta K / K)^2,$$

where  $\chi$  is the crystal susceptibility,  $B \sim B_{ijkm}$ , and  $\Delta K \sim \Delta K_{ij}$ . Recognizing that  $u_{ij} \sim \beta \Delta T$ , where  $\beta$  is the crystal thermal-expansion coefficient, and putting

$$\chi \sim 10^{-3}, \quad B = 10^7 \text{ erg/cm}^3, \quad \Delta T \approx 1 \text{ K}, \quad H_a \approx 7 \cdot 10^3 \text{ G},$$

$$H = 300 \text{ G}, \quad 4\pi M_s = 30 \text{ G}, \quad \beta = 10^{-5} \text{ K}^{-1},$$

we get

$$\Delta K / K = 10^{-2}, \quad \Delta M_{me}^{(1)} \approx 3 \cdot 10^{-2} \text{ G}, \quad \Delta M_{me}^{(2)} \approx 6 \cdot 10^{-4} \text{ G}.$$

At film thicknesses  $h \approx 4.8 \mu\text{m}$  and  $R \approx a \approx 1$  this corre-

sponds to  $\mathcal{E} \sim 10^{-5} \text{ V}$ , which is smaller by an order of magnitude than the experimental emf signals.

If the emf is proportional to the derivative of the intensity, we shall speak, in accordance with the foregoing, of a direct light-induced change of the magnetization. If, however, the emf is proportional to the intensity, we shall speak arbitrarily of a thermal mechanism but bear in mind that such a dependence can occur also in the direct mechanism if the magnetization relaxation time is long.

#### 4. MEASUREMENT RESULTS

For the batch of crystals with  $R = \text{Lu}$  we observed the bipolar emf signal typical of the direct mechanism (see Fig. 1 of Ref. 18). We note the following important point: the polarity of emf signal corresponded to an increase of the crystal magnetization by the light, meaning  $\kappa > 0$  in Eq. (5). The signal amplitude remained the same within the limits of experimental error ( $\approx 15\%$ ) when a change to circular polarization was made. This remark pertains also to all the crystals investigated in our present study.

The plot of the signal amplitude vs the external magnetic field is close to the magnetization curve  $M(H)$ .<sup>18</sup> This means that the observed change of the crystal magnetization is proportional to the initial magnetization. The dependence of the signal emf amplitude on the laser-radiation power was linear,<sup>18</sup> thus confirming the statements made in Sec. 2 concerning the mechanisms that alter the magnetization. This linear dependence allows us also to state that the influence of two-photon absorption on the light-induced magnetization, which was observed in Ref. 24, can be neglected under our conditions.

For films  $10 \mu\text{m}$  thick, with a saturation magnetization  $4\pi M_s = 100 \text{ G}$  and an absorption coefficient  $\alpha \approx 10\text{--}15 \text{ cm}^{-1}$ , the signal amplitude per turn of coil in the region of saturating magnetic fields was  $\approx 0.18 \text{ mV/MW}$ . The heat rise of the sample in the illuminated region did not exceed  $1 \text{ K}$  in this case. With rise of temperature, the lower peak increased in amplitude, "crawled" over the positive peak, which it ultimately exceeded and suppressed completely. Thus, with rise of temperature the direct light-induced magnetization mechanism is replaced by the thermal one, in which the form of the signal emf is practically equal to the form of the laser pulse, and the light-induced magnetization decreases the initial magnetization of the crystal. The quali-

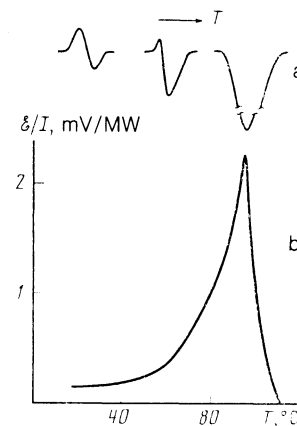


FIG. 1. Temperature dependence; a—of the emf signal form; b—of the amplitude of the negative emf peak. Sample with  $R = \text{Lu}$ ,  $h = 10 \mu\text{m}$ .

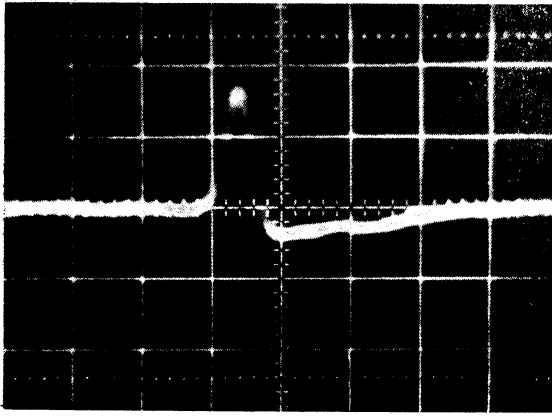


FIG. 2. Signal emf for sample with R = Lu,  $h = 4.8 \mu\text{m}$  (at  $\tau_L \approx 7 \text{ ns}$ ). Sweep 10 ns/div.

tative temperature dependence of the amplitude of the signal is shown in Fig. 1. The steep increase of the amplitude to 2–3 mV/MW in the  $T \approx 100^\circ\text{C}$  region can be attributed to the approach to the Curie point  $T_C$ , where the derivative  $\partial M / \partial T$  increases. At  $T > T_C$  the signal from the coil vanished completely.

For samples with R = Lu,  $4.8 \mu\text{m}$  thick and with saturation magnetization  $4\pi M_s \approx 30 \text{ G}$ , the amplitude of the negative maximum at room temperature was approximately one-quarter of the positive-maximum amplitude which reached 0.25 mV/MW (Fig. 2). This case can be interpreted as due to the direct mechanism of light-induced magnetization at  $\tau \approx \tau_L$ .

A similar picture was observed for films with R = Yb of thickness  $3.5 \mu\text{m}$ : the negative spike was 1/3–1/4 of the positive. The amplitude of the positive peak of the signal was  $\approx 0.1 \text{ mV/MW}$  per turn of the coil. The plots of the emf vs the external field and the laser-pulse energy were similar to those described above. Temperature measurements have shown that the maximum signal is reached at  $T \approx 95\text{--}100^\circ\text{C}$  and equals  $\approx 0.6 \text{ mV/MW}$ , noticeably less than the maximum signal for the  $10\text{-}\mu\text{m}$  film with R = Lu.

We investigated also a batch of crystals with R = Tm, containing different additives (Bi, Ga) and having greatly differing absorption coefficients  $\alpha \approx 20\text{--}300 \text{ cm}^{-1}$ ; the variation is apparently due to different contents of micro-impurities, such as Pb, which penetrate into the film from the initial melt during the epitaxy. For strongly absorbing films with  $\alpha \approx 300 \text{ cm}^{-1}$  and thickness  $20 \mu\text{m}$ , a large thermal signal was observed, corresponding to a decrease of the initial magnetization. The signal amplitude was  $\approx 2.4 \text{ mV/MW}$  at room temperature and reached  $\approx 10 \text{ mV/MW}$  when the temperature was raised to  $T_C = 140^\circ\text{C}$ . No signal whatever was obtained from another sample having R = Tm,  $6.5 \mu\text{m}$  thick and with  $\alpha \approx 20 \text{ cm}^{-1}$ . On heating to  $T_C$ , a signal of thermal form appeared. Signals of thermal form only were observed also for a batch of samples with R = (Lu, Sm) of thickness  $\approx 15 \mu\text{m}$  and with  $\alpha \approx 100 \text{ cm}^{-1}$ .

## 5. OPTICAL MAGNETIZATION

We proceed now to a theoretical description of direct optical magnetization, in the crystal transparency region, by the change of the free energy in the presence of a magnetic field. It follows from the thermodynamic relations<sup>22</sup> that

$$\Delta F_I = -\Delta \epsilon_{ij} E_i E_j^* / 46\pi, \quad (7)$$

where  $\Delta \epsilon_{ij}$  is the dielectric-tensor change due to magnetic ordering and  $E$  is the light-wave electric-field amplitude. We are interested here in the magnetization connected with the symmetric part  $\Delta \epsilon_{ij}^s$ , since effects connected with the anti-symmetric part have been considered in Refs. 2–6.

Iron-garnet crystals are three-sublattice ferrimagnets. At room temperatures, however, when the condition  $T \gg T_R$  are always met ( $T_R$  is the Curie temperature of the rare-earth sublattice), the sublattice magnetization can be neglected. This is all the more true for samples containing the nonmagnetic  $\text{Lu}^{3+}$  ions. In this case a contribution to the magnetization will always be made by the octahedral (a) and tetrahedral (d) iron sublattices.

For cubic crystals, the symmetric part of the free energy of a ferromagnet with two nonequivalent sublattices can be written in the form<sup>25</sup>

$$\begin{aligned} -16\pi \Delta F_I^s = & \sum_{A=a,d} \left\{ (\mathbf{E}\mathbf{E}^*) \left[ \mathbf{M}^{A2} Q_{12}^{AA} + 2(\mathbf{M}^A \mathbf{H}) Q_{12}^{AH} \right. \right. \\ & + 2 \sum_{B \neq A} (\mathbf{M}^A \mathbf{M}^B) Q_{:3}^{AB} \left. \right] + \left[ (\mathbf{M}^A \mathbf{E}) (\mathbf{M}^A \mathbf{E}^*) Q_{44}^{AA} \right. \\ & + 2(\mathbf{M}^A \mathbf{E}) (\mathbf{H}\mathbf{E}^*) Q_{44}^{AH} + 2 \sum_{B \neq A} (\mathbf{M}^A \mathbf{E}) (\mathbf{M}^B \mathbf{E}^*) Q_{44}^{AB} + \text{c.c.} \left. \right] \\ & + \sum_{\alpha=1}^3 |\mathbf{E}_\alpha|^2 \left( M_\alpha^{A2} \bar{Q}^{AA} + 2M_\alpha^A H_\alpha \bar{Q}^{AH} + 2 \sum_{B \neq A} M_\alpha^A M_\alpha^B \bar{Q}^{AB} \right) \left. \right\} \\ & \bar{Q}^{AB} = Q_{44}^{AB} - Q_{12}^{AB} - 2Q_{44}^{AB}. \quad (8) \end{aligned}$$

Here  $\mathbf{M}^{a,d}$  are the total magnetizations of the octahedral and tetrahedral sublattices, respectively,  $Q_{ij}$  are the conventional symbols for the fourth-rank tensors  $Q_{ijkl}$  (Ref. 25), and  $Q_{ij}^{AH}$  are the components of the tensor connected with the contribution of the field terms. The quantities  $(Q_{11} - Q_{12})$  and  $Q_4$  that enter in  $\bar{Q}$  describe magnetic linear birefringence effects, viz., the direct Cotton-Mouton effect, while the quantities  $\sim Q_{12}$  determine the isotropic magnetic refraction.

The effective magnetic field  $\Delta \mathbf{H}_I$  corresponding to the free energy (8) can be found from the relation

$$\Delta \mathbf{H}_I^A = -\partial \Delta F_I^s / \partial \mathbf{M}^A. \quad (9)$$

Starting from expressions (8) and (9) and from the measurement geometry it is easy to find that the effective magnetic fields  $\Delta \mathbf{H}_I^A$  produced in the magnetic sublattices are parallel to the initial crystal magnetization and proportional to the radiation intensity. The relaxation of the magnetization induced by these fields in the direction of the initial magnetization (longitudinal relaxation) is phenomenologically described by the equation<sup>26</sup>

$$\frac{\partial}{\partial t} \Delta \mathbf{M}_I^A + \frac{\Delta \mathbf{M}_I^A}{\tau_A} = \frac{\chi_A}{\tau_A} \Delta \mathbf{H}_I^A(t). \quad (10)$$

In the derivation of (10) it was assumed that the relaxation of the partial magnetizations is determined only by the effective fields induced by optical radiation in the corresponding sublattices. In Eq. (10),  $\chi_A$  are the differential susceptibilities of the magnetic sublattices:  $\chi_A = \partial \Delta M^A / \partial H$ .

The total change of the magnetization is

$$\Delta M_I = \Delta M_I^a + \Delta M_I^d. \quad (11)$$

Substituting in (10) the expressions (8) and (9) and solving them, we obtain for the partial magnetizations

$$\Delta M_I^A(t) = \frac{M_s^A Q_A}{2cn_0\tau_A} \int_{-\infty}^t \exp\left(-\frac{t-t'}{\tau_A}\right) I(t') dt'. \quad (12)$$

Here  $M_s^A$  are the initial saturation magnetizations of the iron sublattices,  $I = (cn_0/4\pi)(\mathbf{E} \cdot \mathbf{E}^*)$  is the radiation intensity,  $n_0$  is the refractive index of the crystal, and

$$Q_A = Q_{12}^{AH} + \chi_A Q_{12}^{AA} + \chi_B Q_{12}^{AB} + \frac{1}{3}(\tilde{Q}^{AH} + \chi_A \tilde{Q}^{AA} + \chi_B \tilde{Q}^{AB}), \quad A \neq B. \quad (13)$$

Equations (11) and (12) describe the optical magnetization of a two-sublattice ferrimagnet. The effect can be described in the one-sublattice model only in a few limiting cases.

## 6. DISCUSSION OF RESULTS

Let us use the foregoing relations to interpret the experimental results. It was noted above that for films with  $R = \text{Lu}$ ,  $\text{Yb}$  the signal emf is equivalent to the derivative of the form of the laser pulse, and the signal polarity corresponds to an increase of the initial magnetization. With rise of temperature, this signal is replaced by a signal closer in form to the laser pulse, and of opposite polarity, i.e., it corresponds to a decrease of the magnetization.

It follows from the preceding sections that neither the pyromagnetic nor the magnetoelastic (in view the smallness of the latter) mechanisms accounts for the appearance of a bipolar signal emf, since the pyromagnetic signal has a thermal form, and its polarity corresponds to a decrease of the magnetization.

Likewise unrealized in our case is apparently the magnetization-increase mechanism connected with the possible electronic transitions  ${}^6A_{1g} \rightarrow {}^4T_{1g}$  between the ground and first-excited states of the  $\text{Fe}^{3+}$  ion in an octahedral sublattice. In the latter case the recorded signal emf should, in view of the long lifetime of the  $\text{Fe}^{3+}$  ion in the  ${}^4T_{1g}$  state ( $\sim 10^{-6}$  s) at  $T \approx 300$  K (Ref. 28), also agree in form with the laser pulse, and its amplitude should increase with rise of the temperature,<sup>29</sup> something not observed in experiment.

We reach thus the conclusion that the negative spike of the bipolar signal emf is due to superposition of signals due to the action of both a pyromagnetic and a direct optical mechanism (ICME), the form of the latter being determined by longitudinal relaxation of the magnetization. In "pure" form, the ICME was conserved for samples with  $R = \text{Lu}$ ,  $h = 8 \mu\text{m}$ , and  $R = \text{Yb}$ ,  $h = 3.5 \mu\text{m}$  (Fig. 2). Reduction of the measurement results, with allowance for Eq. (4), has made it possible to estimate the relaxation time of the optical magnetization at  $\tau = 34 \pm 6$  ns. This value is of the same order as  $\tau \approx 10^{-7}$  s given in Ref. 26. On the contrary, for samples with  $R = \text{Lu}$ ,  $h = 10 \mu\text{m}$  one observes a bipolar almost-symmetrical signal emf which is a superposition of the ICME signal and of a negative thermal signal comparable in magnitude with the ICME. The lesser role of

the pyromagnetism for the first two samples is attested to also by the fact that they have a smaller thermal-signal amplitude in the vicinity of the Curie point.

We present now numerical estimates of the effective components  $Q^{MM}$  and  $Q^{MH}$  that determine the contribution made to the induced magnetization of the crystal. We use to this end data for Lu films:

$$\chi = 10^{-3}, \quad n_0 = 2.3, \quad 4\pi M_s = 30 \text{ G}, \quad h = 4.8 \mu\text{m}.$$

The induced magnetization  $\Delta M_I$  amounts for the foregoing parameters to 0.26 G. In addition, we take it into account that at temperatures far from the Curie point we can use the relations<sup>30</sup>

$$M_s^d/M_s^a \approx \chi_d/\chi_a = (3 - 0.9x)/(2 - 0.1x),$$

where  $x$  is the density of the  $\text{Ga}^{3+}$  ions for samples with  $4\pi M_s = 30$  G. We use also  $\tau_d \approx \tau_a$  in the estimates. Assuming then that the contributions of the isotropic terms are much larger than the anisotropic ones,  $Q_{12} \gg Q_1$ , we obtain from the experimental value of the direct magnetization the estimate

$$Q = Q_{12}^{MH} + \chi Q_{12}^{MM} \approx 2 \cdot 10^{-4} \text{ G}^{-2}.$$

Here

$$\chi = \chi_a + \chi_d, \quad Q_{12}^{MH} \approx 32(Q_{12}^{dH} - Q_{12}^{aH}), \\ Q^{MM} \approx 60(Q_{12}^{dd} - Q_{12}^{aa}).$$

This yields, assuming that the contribution of the field terms to  $Q$  is small, an estimate of the isotropic change of the refractive index,  $\Delta n_0 \approx 0.08$ , which differs by one or two orders of magnitude from the experimental data.<sup>31</sup> It must therefore be assumed that the obtained value of  $Q$  is determined by the contribution of field terms  $\sim Q^{AH}$ . Similar results on the antisymmetric part of the dielectric constant were obtained in Ref. 20, which is devoted to an investigation of the field dependence of the Faraday-rotation angle on the external magnetic field.

It is necessary therefore to refine the results of Ref. 6, which deals with the IFE in magnetically ordered crystals, by including the field terms in the analysis. This leads to the following equation for the magnetization change to the antisymmetric part of  $\Delta \epsilon^a$ :

$$\Delta M_\phi = \frac{cn_0 i [\mathbf{E} \mathbf{E}^*]}{2\pi\omega} (K^{MH} + \chi K^{MM}).$$

Here  $K^{MH}$  is the kund constant, which determines the field dependence of the Faraday rotation angle of the polarization plane. If all the foregoing is valid also for the relations between the constants  $K^{MH}$  and  $\chi K^{MM}$ , the theoretical estimate of the value is substantially increased.

We note in conclusion that we did not succeed in observing the IFE. The apparent reason is that in our experimental geometry the main contribution to the ICME is made by an isotropic field term. This term is larger by one or two orders than the anisotropic spin-orbit terms which are the same order of magnitude for the IFE and the ICME. It should be noted that in the Cotton-Mouton geometry, in which the

external field  $h$  lies in the sample plane, the contribution of the isotropic term to the magnetization vanishes and it may be possible to observe the anisotropic terms both in the ICME and in the IFE.

- <sup>1</sup>V. F. Kovalenko and É. L. Nagaev, *Usp. Fiz. Nauk* **148**, 561 (1986) [*Sov. Phys. Usp.* **29**, 297 (1986)].
- <sup>2</sup>L. P. Pitaevskii, *Zh. Eksp. Teor. Fiz.* 1450 (1960) [*Sov. Phys. JETP* **12**, 1008 (1960)].
- <sup>3</sup>P. S. Pershan, *Phys. Rev.* **130**, 919 (1963).
- <sup>4</sup>P. S. Pershan, J. P. van der Ziel, and L. D. Malmstrom, *ibid.* **143**, 574 (1966).
- <sup>5</sup>B. A. Zon and Yu. N. Mitin, *Zh. Eksp. Teor. Fiz.* **78**, 1718 (1980) [*Sov. Phys. JETP* **51**, 862 (1980)].
- <sup>6</sup>B. A. Zon and V. Ya. Kupershmidt, *ibid.* **84**, 363 (1983) [**57**, 363 (1983)].
- <sup>7</sup>B. A. Zon and V. Ya. Kupershmidt, *Fiz. Tverd. Tela (Leningrad)* **25**, 1231 (1983) [*Sov. Phys. Solid State* **25**, 708 (1983)].
- <sup>8</sup>J. P. Van der Ziel and N. Bloembergen, *Phys. Rev.* **138**, 1287 (1965).
- <sup>9</sup>G. M. Genkin and I. D. Tokman, *Zh. Eksp. Teor. Fiz.* **82**, 1532 (1982) [*Sov. Phys. JETP* **55**, 887 (1982)].
- <sup>10</sup>G. M. Genkin, Yu. N. Nozdrin, I. D. Tokman, and V. N. Shastin, *Pis'ma Zh. Eksp. Teor. Fiz.* **35**, 162 (1982) [*JETP Lett.* **35**, 199 (1982)].
- <sup>11</sup>K. Kubota, *Sol. St. Comm.* **10**, 633 (1972).
- <sup>12</sup>V. G. Guzhva, Yu. V. Koltok, V. M. Kuzymichev, and Yu. M. Latynin, *Kvant. Electron. (Moscow)* **4**, 681 (1977) [*Sov. J. Quant. Electron.* **7**, 384 (1977)].
- <sup>13</sup>A. M. Balbashov, B. A. Zon, V. Ya. Kupershmidt, *et al.*, *Fiz. Tverd. Tela (Leningrad)* **26**, 1297 (1987) [*Sov. Phys. Solid State* **26**, 790 (1987)].
- <sup>14</sup>J. E. Holzrichter, R. M. Macfarlane, and A. L. Schawlow, *Phys. Rev. Lett.* **26**, 652 (1971).
- <sup>15</sup>M. M. Afanas'ev, M. E. Kompan, and I. A. Merkulov, *Pis'ma v Zh. Tekh. Fiz.* **2**, 982 (1976) [*Sov. Tech Phys. Letters* **2**, 385 (1976)].
- <sup>16</sup>V. G. Veselago, S. G. Rudov, and M. A. Chernikov, *Pis'ma Zh. Eksp. Teor. Fiz.* **40**, 181 (1984) [*JETP Lett.* **40**, 940 (1984)].
- <sup>17</sup>E. Z. Katsnelson and A. G. Karoza, *Phys. St. Sol. (a)* **90**, K49 (1985).
- <sup>18</sup>B. A. Zon, V. Ya. Kupershmidt, G. V. Pakhomov, and T. T. Urazbaev, *Pis'ma Zh. Eksp. Teor. Fiz.* **45**, 219 (1987) [*JETP Lett.* **45**, 272 (1987)].
- <sup>19</sup>R. V. Pisarev, J. Schoenes, and P. Wachter, *Sol. St. Comm.* **23**, 657 (1977).
- <sup>20</sup>U. V. Valiev, A. K. Zvesdin, G. S. Krinchik, *et al.*, *Zh. Eksp. Teor. Fiz.* **85**, 311 (1983) [*Sov. Phys. JETP* **58**, 181 (1983)].
- <sup>21</sup>R. Serov, M. C. Richardson, and P. Burtyn, *Rev. Sci. Instr.* **46**, 866 (1975).
- <sup>22</sup>L. D. Landau and E. M. Lifshitz, *Electrodynamics of Continuous Media*, Pergamon, 1984, Chap. 4, p. 30.
- <sup>23</sup>S. Krupicka, *Physics of Ferrites and Related Magnetic Oxides* [Russ. transl.], Mir, 1976, Vol. 2, Chap. 1.
- <sup>24</sup>S. I. Shabaev and R. V. Pisarev, *Pis'ma Zh. Eksp. Teor. Fiz.* **45**, 490 (1987) [*JETP Lett.* **45**, 626 (1987)].
- <sup>25</sup>*Dynamic and Kinetic Properties of Magnets* [in Russian], S. V. Vonsovskii and E. A. Turov, eds., Nauka, 1986, Chap. 2.
- <sup>26</sup>A. I. Akhiezer, V. G. Bar'yakhtar, and S. V. Peletminskii, *Spin Waves*, Wiley, 1969.
- <sup>27</sup>B. B. Kravtsov, O. Ochilov, and R. V. Pisarev, *Fiz. Tverd. Tela (Leningrad)* **25**, 2404 (1983) [*Sov. Phys. Solid State* **25**, 1380 (1983)].
- <sup>28</sup>G. M. Genkin, I. D. Tokman, and V. V. Zil'bergen, *Sol. St. Comm.* **44**, 631 (1982).
- <sup>29</sup>D. L. Wood and J. P. Remeika, *J. Appl. Phys.* **38**, 1038 (1967).
- <sup>30</sup>A. Eschenfelder, *Physics and Technology of Bubble Domains* [Russ. Transl.], Mir, 1983, 6.2.2.
- <sup>31</sup>T. Ferre and G. A. Gehring, *Rep. Prog. Phys.* **47**, 513 (1984).

Translated by J. G. Adashko